

Supporting Information for

## Obtaining the Phenomenological Rate Coefficients to Describe the Decomposition Kinetics of Corannulene Oxyradical at High Temperatures

Hongmiao Wang,<sup>ab</sup> Xiaoqing You,<sup>ab\*</sup> Mark Blitz,<sup>c</sup> Michael J Pilling,<sup>c</sup>  
Struan H Robertson<sup>d\*</sup>

<sup>a</sup>Center for Combustion Energy, Tsinghua University, Beijing, 100084, China

\*Corresponding author: [xiaoqing.you@tsinghua.edu.cn](mailto:xiaoqing.you@tsinghua.edu.cn)

<sup>b</sup>Key Laboratory for Thermal Science and Power Engineering of Ministry of  
Education, Tsinghua University, Beijing 100084, China

<sup>c</sup>School of Chemistry, University of Leeds, Leeds, U.K.

<sup>d</sup>Dassault Systèmes, BIOVIA, 334, Cambridge Science Park, Cambridge, U.K., CB4 0WN

\*Corresponding author: [struanhrobertson@gmail.com](mailto:struanhrobertson@gmail.com)

In this supporting information, we present:

### 1. Analysis of the microcanonical equilibration between species f and f5

- **Figure S1.** Concentration profiles of corannulene oxyradical decomposition from master equation modelling over 1500 – 2500 K at (a) 0.1 atm, (b) 1 atm, (c) 10 atm, — complete system, --- reduced system.
- **Figure S2.** Concentration ratios of f5 and f over 0.1 – 1000 atm at 2000 K from the master equation modelling of corannulene oxyradical f decomposition.
- **Figure S3.**  $\ln \left( \frac{[f] - [f_{eq}]}{1 - [f_{eq}]} \right)$  as a function of time during the isomerization between f and f5 at 2500 K and 1 atm from the master equation modelling of corannulene oxyradical f decomposition.

### 2. Analysis of the time dependence of the effective rate constants

- **Figure S4.**  $\ln ([f'])$  as a function of time at 2500 K and 0.1 atm from the master equation modelling of the reduced system of corannulene oxyradical f' decomposition.
- **Figure S5.** Temperature and pressure dependence of the rate coefficients of the reduced system of corannulene oxyradical f' decomposition over 1500-2500 K and 0.1 - 10 atm, (a) 0.1 atm, (b) 1 atm, (c) 10 atm, (d) eigenvalue method, (e) 1/e method, (f) fitting method.

- **Figure S6** The eigenvalue spectra and the effective rate coefficients obtained by optimal fitting method from the master equation modelling of the reduced system of corannulene oxyradical f' decomposition at (a) 1 atm and (b) 10 atm over 1500-2500 K.

### 3. Analysis of the reverse rate coefficients

- **Figure S7.** Comparisons of species profiles of the modified system of corannulene oxyradical f' decomposition at 2500 K, 0.1 atm, — reversible master equation modelling, --- kinetic modelling based on the thermodynamics method. — kinetic modelling based on the relaxation rate constant method, ... kinetic modelling based on the combined method.
- **Table S1.** Comparison of the forward and reverse rate constants of the modified system of corannulene oxyradical f' decomposition at 2500 K and 0.1 atm using different methods.

### 4. Analysis of the size effect of oxyradicals

- **Figure S8.** Boltzmann distributions and mean collision frequencies of phenoxy, oxyradical f and oxyradical g at (a) 1500 and (b) 2500 K, as well as the microcanonical isomerization rate coefficients. Isomerization thresholds of phenoxy, oxyradical f and oxyradical g are 50.8 kcal/mol, 47.2 kcal/mol and 57.4 kcal/mol respectively.
- **Table S2.** Effective rate coefficients calculated by different methods for thermal decomposition of phenoxy, oxyradical f' and oxyradical g at 1500-2500 K, 0.1 atm.

## 1. Analysis of the microcanonical equilibration between species f and f5

The rate equation for the production of f3 can be expressed as

$$\frac{dx_{f3}}{dt} = k_{f5-f3} x_{f5} \quad (1)$$

The RRKM microcanonical rate constant for reactive loss via  $TS_{5-3}$  is given by

$$k_{f5-f3}(E) = \frac{W_{f5-f3}^{\dagger}(E)}{h\rho_{f5}(E)} \quad (2)$$

If there is fast conversion between f and f5 at short times, we assume that f and f5 are in microcanonical equilibrium, and consequently, at the microcanonical level, we have

$$\frac{x_f(E)}{\rho_f(E)} = \frac{x_{f5}(E)}{\rho_{f5}(E)} \quad (3)$$

Under these conditions the species f and f5 essentially behave as a single species, f', and the population of this single species is:

$$x_{f'}(E) = x_f(E) + x_{f5}(E) \quad (4)$$

It follows from Eq. (3) that

$$x_{f'}(E) = x_{f5}(E) \left( \frac{\rho_f(E)}{\rho_{f5}(E)} + 1 \right) \quad (5)$$

and so,

$$\frac{x_{f'}(E)}{\rho_f(E) + \rho_{f5}(E)} = \frac{x_{f5}(E)}{\rho_{f5}(E)} \quad (6)$$

The rate equation of the new reaction  $f' \leftrightarrow f3$  is simply related to Eq. (1):

$$\frac{dx_{f'}}{dt} = - \frac{dx_{f3}}{dt} \quad (7)$$

Combining (1) and (7), at an energy level E, we have

$$\frac{dx_{f'}(E)}{dt} = - k_{f5-f3}(E) x_{f5}(E) \quad (8)$$

Substituting Eq. (2) into Eq. (8), we get

$$\frac{dx_{f'}(E)}{dt} = - \frac{W_{f5-f3}^{\dagger}(E) x_{f5}(E)}{h\rho_{f5}(E)} \quad (9)$$

Combining Eqs. (6) and (9) gives,

$$\frac{dx_{f'}(E)}{dt} = - \frac{W_{f5-f3}^{\dagger}(E)}{h\rho_f(E)} x_{f'}(E) = - \frac{W_{f5-f3}^{\dagger}(E)}{h(\rho_f(E) + \rho_{f5}(E))} x_{f'}(E) \quad (10)$$

Hence, an equation of motion for the combined species f' is obtained, with an effective rate coefficient,  $k_{eff}$ , of,

$$k_{eff} = \frac{W_{f5-f3}^\dagger(E)}{h(\rho_f(E) + \rho_{f5}(E))} \quad (11)$$

This rate coefficient applies under the assumption that f and f5 are in rapid microcanonical equilibrium in the zero pressure limit. At higher pressures, collisions will alter the relative distribution and f and f5 may not be in microcanonical equilibrium.

Alternatively, we may analyze the system via eigenvalues. The coupled equations for f and f5 at a fixed energy E with no collisions are as follows:

$$\frac{dc}{dt} = \begin{pmatrix} -k_{f-f5}(E) & k_{f5-f}(E) \\ k_{f-f5}(E) & -k_{f5-f}(E) - k_{f5-f3}(E) \end{pmatrix} c = \begin{pmatrix} -A & B \\ A & -C \end{pmatrix} c \quad (12)$$

where  $c = \begin{pmatrix} [f(E)] \\ [f5(E)] \end{pmatrix}$

There are two eigenvalues from the transition matrix, which lead to the analytic solutions of the concentration evolution of the species with time:

$$\lambda_{\pm} = \frac{-(A+C) \pm \sqrt{(A+C)^2 - 4A(C-B)}}{2} = \frac{-(A+C)}{2} \left[ 1 \mp \left( 1 - \frac{4A(C-B)}{(A+C)^2} \right)^{1/2} \right] \quad (13)$$

Because  $(A+C)^2 \gg 4A(C-B)$ , to a good approximation, we obtain:

$$\lambda_- = -(A+C) + \frac{A(C-B)}{A+C} \approx -(k_{f-f5}(E) + k_{f5-f}(E) + k_{f5-f3}(E)) \quad (14)$$

$$\lambda_+ = -\frac{A(C-B)}{A+C} = -\frac{k_{f-f5}(E)k_{f5-f3}(E)}{k_{f-f5}(E) + k_{f5-f}(E) + k_{f5-f3}(E)} \quad (15)$$

The numerically larger eigenvalue,  $\lambda_-$ , governs the (rapid) equilibration of f and f5, while the numerically smaller one,  $\lambda_+$ , corresponds to the decay of the equilibration mixture of f and f5, namely, f'.

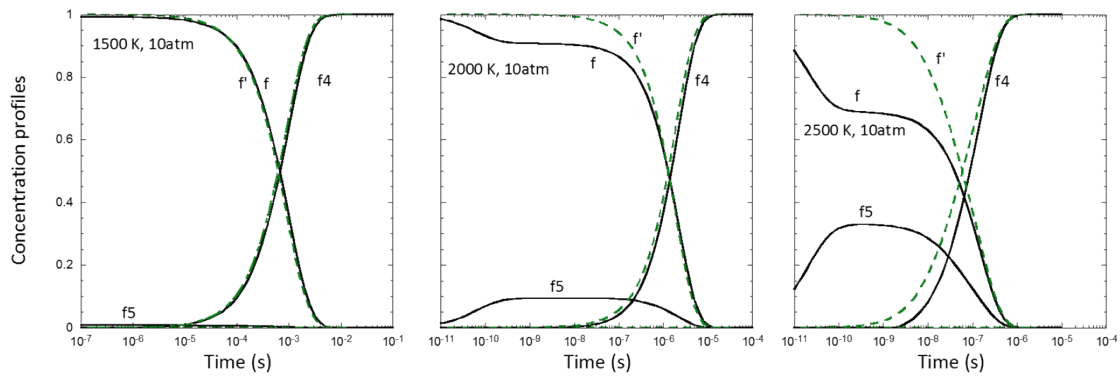
If the inequalities,  $k_{f-f5}(E) \gg k_{f5-f3}(E)$ ,  $k_{f5-f}(E) \gg k_{f5-f3}(E)$ , (which imply that f and f5 rapidly achieve microcanonical equilibrium) apply, and the RRKM microcanonical rate constant equation substituted into Eq. (15), we get:

$$\lambda_+ \approx -\frac{k_{f-f5}(E)k_{f5-f3}(E)}{k_{f-f5}(E) + k_{f5-f}(E)} = -\frac{W_{f5-f3}^\dagger(E)}{h(\rho_f(E) + \rho_{f5}(E))} \quad (16)$$

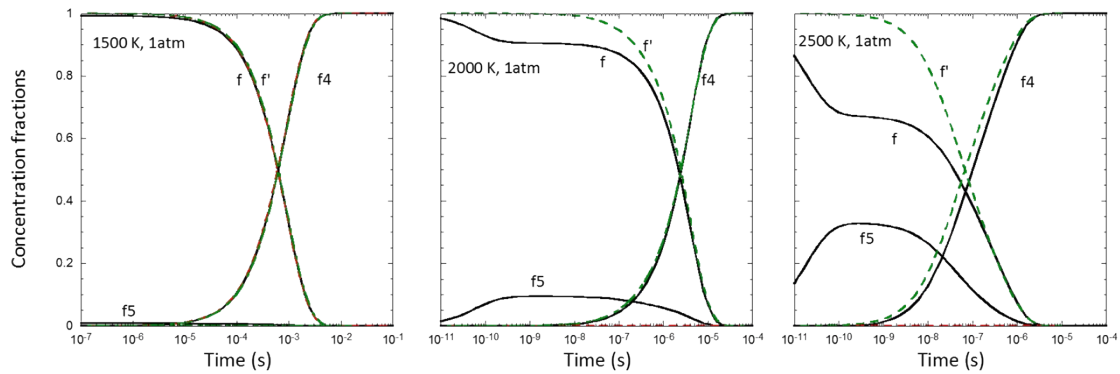
We can identify this eigenvalue with the rate coefficient for the decay of the combined species  $f'$  (which has a density of states of  $\rho_f(E) + \rho_{f5}(E)$ ) and write the rate equation as:

$$\frac{dx_{f'}(E)}{dt} = -\frac{W_{f5-f3}^{\dagger}(E)}{h(\rho_f(E) + \rho_{f5}(E))} x_{f'}(E) \quad (17)$$

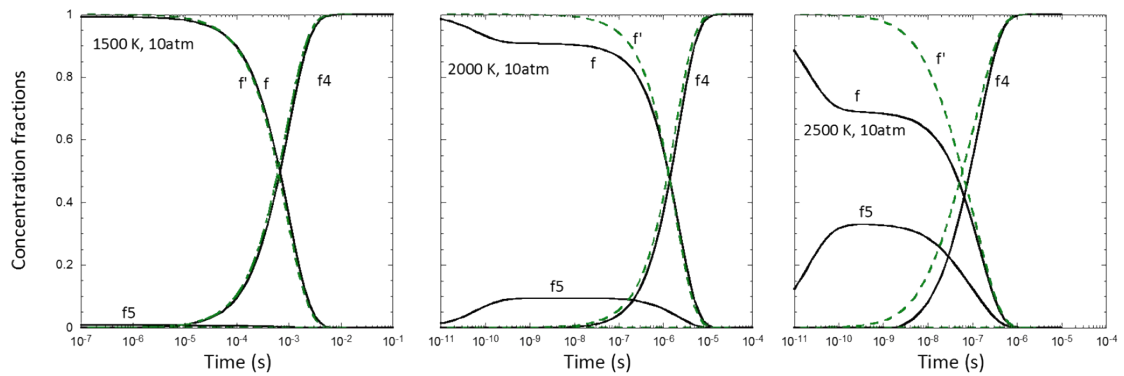
Eq. (17) is identical to Eq. (10).



(a)



(b)



(c)

**Figure S1** Concentration profiles of corannulene oxyradical decomposition from master equation modelling over 1500 – 2500 K at (a) 0.1 atm, (b) 1 atm, (c) 10 atm, — complete system, --- reduced system.

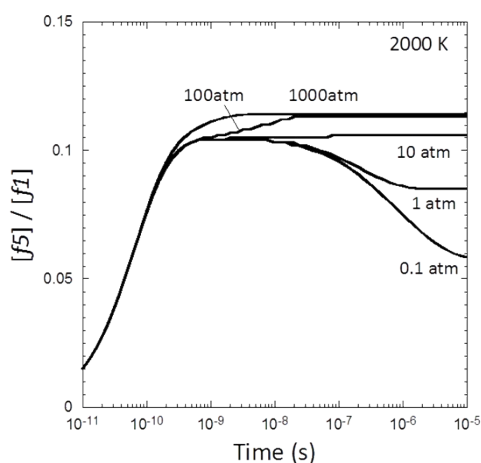


**Figure S2** Concentration ratios of f5 to f at 2000 K over 0.1 – 1000 atm from the master equation modelling of corannulene oxyradical f decomposition.

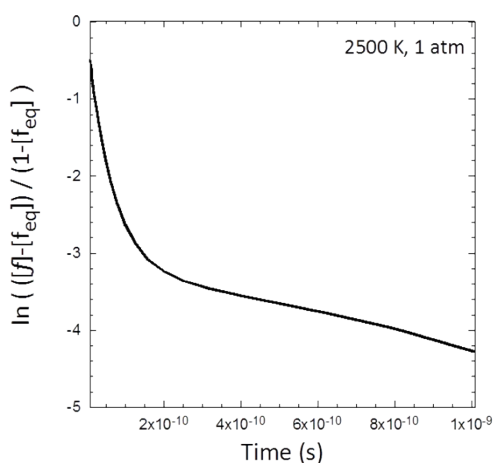


**Figure S3**  $\ln \left( \frac{[f] - [f_{eq}]}{1 - [f_{eq}]} \right)$  as a function of time during the isomerization between f and f5 at 2500 K and 1 atm from the master equation modelling of corannulene oxyradical f decomposition.

The concentration profiles from the master equation modeling of corannulene oxyradical decomposition show that f and f5 approach a steady state on a very short time scale ( $\sim 10^{-10} - 10^{-9}$  s), during which collisions are insignificant to produce relaxation.  $[f_{eq}]$  is the concentration of f at the time of  $10^{-9}$  s. The significant curvature of the plot of  $\ln \left( \frac{[f] - [f_{eq}]}{1 - [f_{eq}]} \right)$  as a function of time indicates that the time dependence of the isomerization of f and f5 is non-exponential.

## 2. Analysis of the time dependence of the effective rate constants

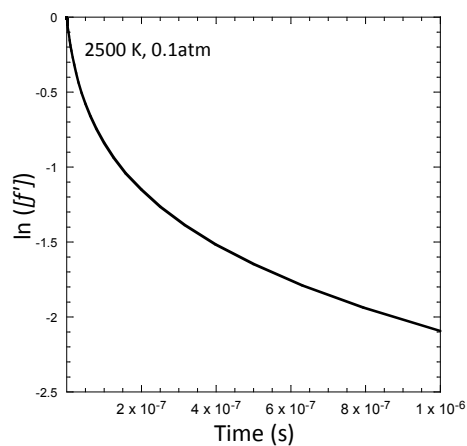


**Figure S4**  $\ln([f'])$  as a function of time at 2500 K and 0.1 atm from the master equation modelling of the reduced system of corannulene oxyradical  $f'$  decomposition.

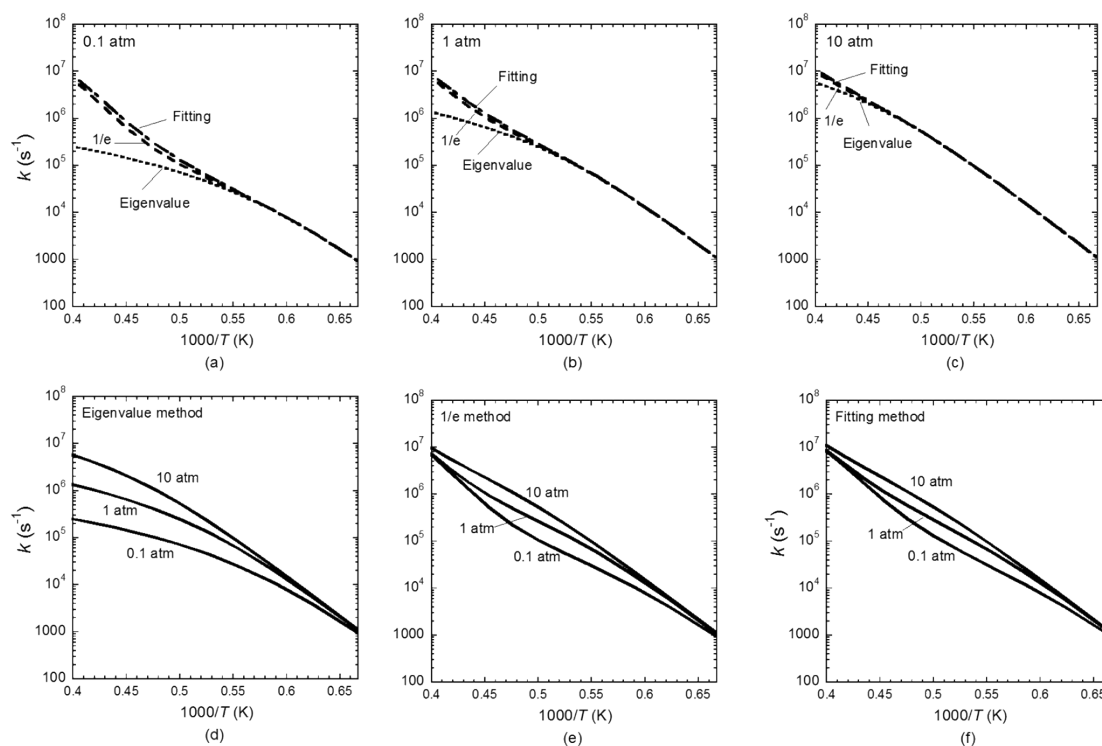


**Figure S5** Temperature and pressure dependence of the rate coefficients of the reduced system of corannulene oxyradical  $f'$  decomposition over 1500-2500 K and 0.1 - 10 atm, (a) 0.1 atm, (b) 1 atm, (c) 10 atm, (d) eigenvalue method, (e) 1/e

method, (f) fitting method.

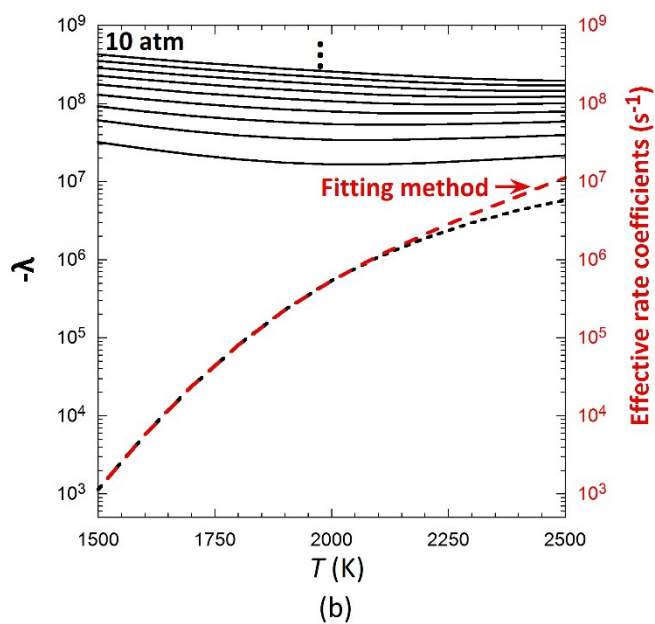
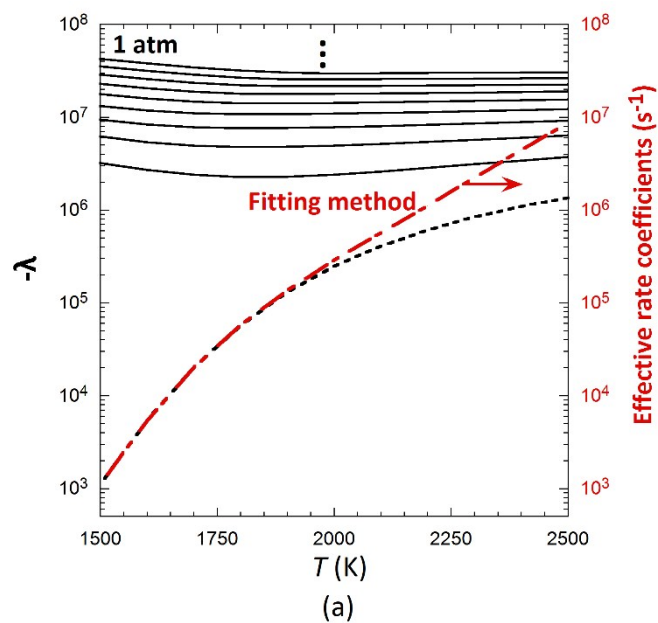


**Figure S6** The eigenvalue spectra and the effective rate coefficients obtained by optimal fitting method from the master equation modelling of the reduced system of corannulene oxyradical  $P'$  decomposition at (a) 1 atm and (b) 10 atm, 1500-2500 K.



### 3. Analysis of the reverse rate coefficients

To demonstrate more clearly the effect of overlapping eigenvalues on the reverse rate constants, the potential energy was modified by increasing the product energy by 25 kcal/mol as shown in the following (units: kcal/mol) and referred to as the modified system hereafter. Note that the intermediate f3 was ignored in the system since it does not have a significant influence on the overall kinetics due to its very shallow well.

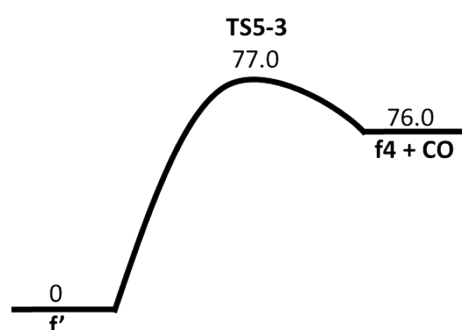


**Table S1.** Comparison of the forward and reverse rate coefficients of the modified system of  $f'$  decomposition at 2500 K and 0.1 atm using different methods.

Method	$k_f$ ( $s^{-1}$ )	$k_r$ ( $cm^3 mol^{-1} s^{-1}$ )
Thermodynamics Method	$8.3 \times 10^6$	$6.7 \times 10^{10}$
Relaxation Method	$8.3 \times 10^6$	$1.1 \times 10^{11}$
Combined Method	$9.0 \times 10^6$	$7.2 \times 10^{10}$

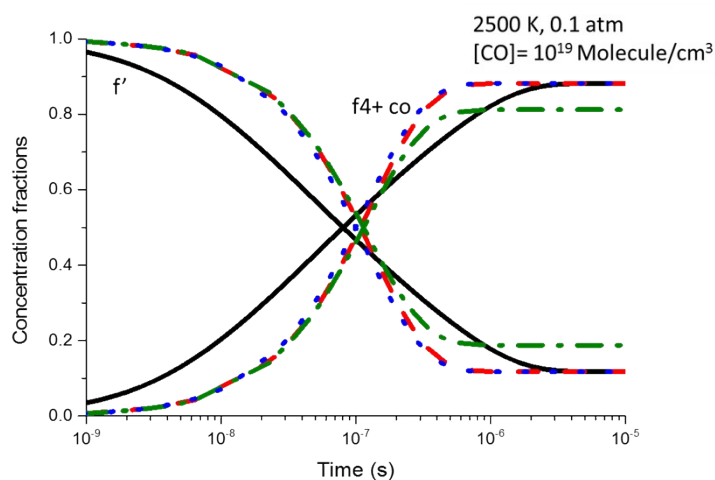


**Figure S7** Comparisons of species profiles of the modified system of corannulene oxyradical  $f'$  decomposition at 2500 K, 1 atm, — reversible master equation modelling, --- kinetic modelling based on the thermodynamics method. —•— kinetic modelling based on the relaxation rate

constant method, ... kinetic modelling based on the combined method.

#### 4. Analysis of the size effect of oxyradicals

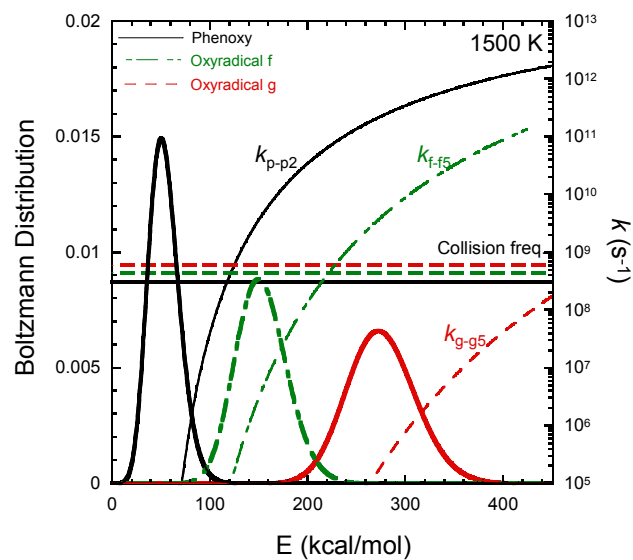
To examine the size effect of oxyradicals, we compare the isomerization and decomposition reactions of oxyradical f with two other oxyradicals of different sizes. One is phenoxy,<sup>1</sup> and the other is a larger oxyradical from our previous work, i.e. oxyradical g.<sup>2</sup> Figure S8 shows the Boltzmann distributions and the mean collision frequencies at (a) 1500 K and (b) 2500 K, as well as the microcanonical reaction coefficients of their first isomerization step along the decomposition pathway as functions of energy. We can see that as the size of oxyradicals increases, the Boltzmann distributions shift significantly to higher energy levels. A direct comparison of the microcanonical rate coefficients for isomerization is difficult, because the threshold energies differ considerably, but the results show the expected slower rise of  $k(E)$  with energy as the radical gets larger. Oxyradical f has the lowest threshold (47.2 kcal/mol) and all the significantly populated states lie to higher energies than the threshold and have higher values for  $k(E)$  than the collision frequency at 2500 K. Phenoxy has a higher threshold (50.8 kcal/mol) but, despite its smaller size, most of the distribution lies above the threshold at 2500 K and many states have rate coefficients higher than the collision frequency at 2500 K. The threshold for oxyradical g is much higher still (57.4 kcal/mol) and, as expected,  $k(E)$  increases more slowly with energy. Even so, all of the significantly populated states lie well above the threshold and the majority have rate coefficients that exceed the collision frequency at 2500 K. Hence, both the high temperature and the large densities of states resulting from the size of radicals, coupled with the low threshold energy for isomerization, have an effect on this type of kinetic behaviour.

Table S2 examines the effective rate coefficients for decomposition of phenoxy and oxyradicals f' and g. The results show that CSE/IERE overlap is significant above 2000 K for all three species, that the kinetics are non-exponential, and that recourse has to be made to effective rate coefficients.

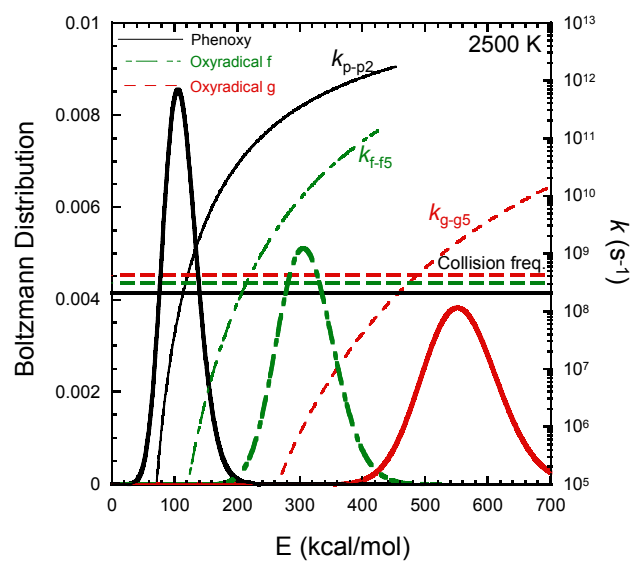
**Table S2.** Effective rate coefficients calculated by different methods for thermal decomposition of phenoxy, oxyradical f' and oxyradical g at 1500-2500 K, 0.1 atm.

Phenoxy			
0.1 atm	Fitting method	Eigenvalue method	Ratio
1500 K	2.6E+04	2.5E+04	1.0
2000 K	5.1E+05	1.8E+05	2.8
2500 K	2.6E+07	3.7E+05	72.4
Oxyradical f'			
0.1 atm	Fitting method	Eigenvalue method	Ratio
1500 K	9.7E+2	9.7E+2	1.0
2000 K	1.3E+5	7.6E+4	1.7
2500 K	8.6E+6	2.7E+5	32.4
Oxyradical g			

0.1 atm	Fitting method	Eigenvalue method	Ratio
1500 K	1.4E+04	1.4E+04	1.0
2000 K	2.6E+06	2.9E+05	8.9
2500 K	1.4E+08	7.0E+05	199.3



(a)



(b)

**Figure S8** Boltzmann distributions and mean collision frequencies of phenoxly, oxyradical f and oxyradical g at (a) 1500 and (b) 2500 K, as well as the microcanonical isomerization rate coefficients. Isomerization thresholds of phenoxly, oxyradical f and oxyradical g are 50.8 kcal/mol, 47.2 kcal/mol and 57.4 kcal/mol respectively.

## References

1. X. Q. You, D. Y. Zubarev, W. A. Lester and M. Frenklach, *J. Phys. Chem. A*, 2011, **115**, 14184-14190.
2. X. You, H. Wang, H.-B. Zhang and M. J. Pilling, *Phys. Chem. Chem. Phys.*, 2016, **18**, 12149-12162.